Dynamic Response of Fixed-base Core-tube and Base-isolated Frame Structure Subjected to Strong Earthquake Motions

Z.D. Yang, E.S.S. Lam

Abstract—Considering the merits and limitations of energy dissipation system, seismic isolation system and suspension system, a new earthquake resistant system is proposed and is demonstrated numerically through a frame-core structure. Base isolators and story isolators are installed in the proposed system. The former "isolates" the frame from the foundation and the latter "separates" the frame from the center core. Equations of motion are formulated to study the response of the proposed structural system to strong earthquake motion. As compared with the fixed-base building system, the proposed structural system shows substantial reduction on structural response.

Keywords—Base Isolator; Core-tube; Isolated frame; Seismic Mitigation; Story Isolator

I. INTRODUCTION

CONVENTIONAL earthquake resistant systems rely on strengthening key structural members to resist the horizontal force due to earthquake and to avoid collapse (e.g. capacity design). Recently, other structural systems have been introduced to reduce the structural response and possible damage by absorbing the earthquake energy and/or counteracting the damaging earthquake. These systems include energy dissipation system, seismic isolation system, and other systems.

Energy dissipation systems are designed to use dampers and corresponding amplification devices to provide supplemental damping to structures [1]-[3]. Commonly used dampers include, but are not limited to, metallic dampers, friction dampers, viscoelastic dampers and fluid dampers [1, 4]. Generally speaking, energy dissipation dampers can increase structures' energy dissipation ability to reduce structural response to earthquakes. However, it has been pointed out by many researchers these dampers have some disadvantages [1]. For example, fluid dampers, viscoelastic dampers and friction dampers may have reliability problems and replacement is necessary for metallic dampers after earthquake [1]. In addition these energy dissipation dampers and corresponding amplification devices can be invasive and may adversely affect the useable floor area.

Seismic isolation systems have been introduced to reduce low-rise buildings' response and possible damage. Generally speaking, seismic isolation systems comprise one or several types of seismic isolators and energy dissipation devices.

Z.D. Yang is a PHD student at the Department of Civil & Structural Engineering, The Hong Kong Polytechnic University, Hung Hom, Hong Kong (phone: 852- 6172 4847; e-mail: 09902640r@connect.polyu.hk).

E.S.S. Lam is with Department of Civil & Structural Engineering, The Hong Kong Polytechnic University, Hung Hom, Hong Kong (e-mail: cesslam@polyu.edu.hk).

These seismic isolators and devices are usually installed between the foundation and base floor to provide small lateral stiffness to shift the building's predominant frequency away from dangerous resonance [5]. Although seismic isolation systems have many successful applications in low-rise buildings, it is usually considered that seismic isolation systems are less effective for high-rise buildings [6]. One reason is seismic isolators are deficient in providing overturning resistance and have limited abilities to bear tensile stresses. Yet, tensile stresses and overturning may occur when a high rise building is under strong earthquakes [7]. Previous observations have also proved the ineffectiveness of seismic isolation systems in high-rise base-isolated buildings. An example is the MT building in Sendai City, a base-isolated high-rise building in Japan. The acceleration data recorded at the 18th floor of this building during the off Miyagi earthquake on May 26, 2003, are larger than ground acceleration [8]. In addition, tall base-isolated buildings could be sensitive to wind excitations which may cause habitability problems [9].

Besides the above mentioned two structural systems, many suspended buildings have been built (e.g. Westcoast transmission building, Vancouver, Library of Tongji University, Shanghai and Standard Bank Centre, Johannesburg), in the past few decades. A suspended building is mainly composed of three parts, namely, main load-bearing part (e.g. one or more core-tube), suspenders (e.g. cantilever or truss) and suspended part. The main load-bearing part provides vertical and lateral resistance capability for the suspension system. Mezzi [10] summarizes three different suspended buildings schemes which are (A) rigid connected system, (B) pin connected system by cable and (C) pin connected system by a balancing beam or truss with cable. Recently a core-suspended isolation system comprising a concrete core and a suspended structure is proposed and constructed in Tokyo, Japan [11]. At the top of the center core is a double layer rubber bearing which supports a suspended frame [11]. Studies on this core-suspended isolation system show response of the suspended part is reduced and the response of the core is amplified [11].

Without connecting to ground, the suspended part of a suspended building can be separated from ground motions and thus improve this part's earthquake behavior. But a suspended building doesn't have multi-defense lines. So, a single failure of one critical member or one joint in the suspender could lead to progressive collapse [12].

Mar and Tipping [13] proposed a smart frame story isolation system which consists of a gravity bearing frame and a lateral load resisting frame. The two frames are connected by an assembly of springs and passive dampers. The smart system can be tuned (e.g. changing the stiffness and damping of the

springs and passive dampers) to optimize the gravity frame's fundamental periods and to reduce the frame's response to earthquake [13].

In this study, a new earthquake resistant system with performance compatible to the above-mentioned systems is proposed. As schematically shown in Fig. 1, the proposed system includes a lateral resisting core-tube and a base-isolated frame. Response of the new system subjected to strong earthquakes is studied as follows.

II. PROCEDURE FOR PAPER SUBMISSION

Representing a simplified thirty storey commercial building, structural scheme of the fixed-base core-tube and base-isolated frame system proposed in this paper is shown in Fig. 1. It is a tube-frame system which comprises a fixed-base reinforced concrete center core and a base-isolated frame at 6 m grids. The fixed-base core-tube and the base-isolated frame are connected at each floor level by story isolators which are replaceable and acting as energy dissipation devices when subjected to winds or earthquakes. Similar energy dissipation method was studied by Luoc and De Barros [14]. They proposed a structural system which comprises a stiff external structure and a flexible internal structure. These two structures are connected by dampers to reduce seismic response [14] by absorbing energies.

Cross-sections of the columns and beams used in this new structural system are 1m×1m and 0.6m×0.6m, respectively. Floor system uses traditional two-way beam-slab construction of 200 mm thickness. Grade C40 concrete is assumed and the Modulus of elasticity is 32.5 GN/m^2. It has a total mass of 3.63×10^4 ton and a total weight of 355.74 MN.

The load transferring mechanism is as follows:

(1) Both the center core and the isolated frame will contribute to transfer the gravity load.

(2) The center core will provide the necessary lateral stiffness to limit the lateral deflection and to prevent possible wind induced oscillation.

(3) Under earthquake action, core-tube will be the principal lateral load resisting system and the frame will be protected by the base isolators. The storey isolators can dissipate energy to reduce response.

III. ANALYTICAL MODEL AND EQUATIONS OF MOTION

It is assumed that the fixed-base core-tube and base-isolated frame structural system is subjected to ground motion in one direction only. Without considering torsional effect, the proposed system can be simplified to a two dimensional model. In the analysis, the core-tube and the frame are assumed to behave linear elastic throughout the loading history.
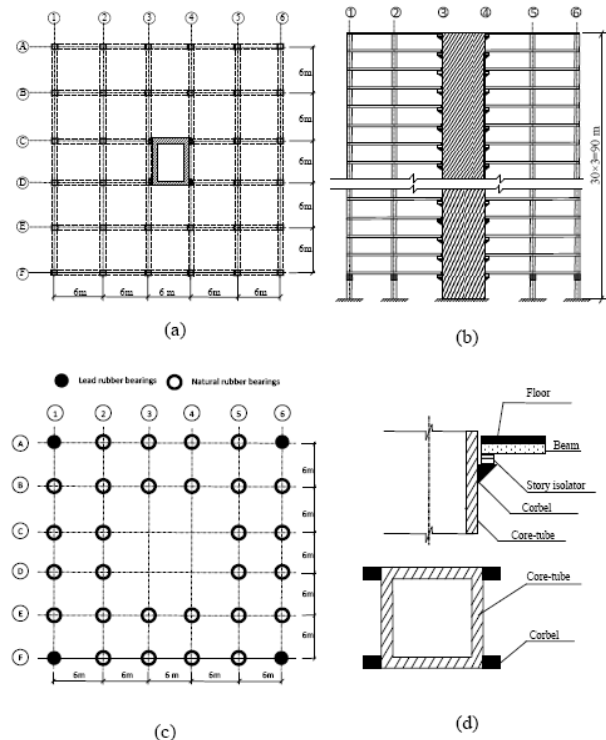

Fig. 1 Arrangement of fixed-base core-tube and base-isolated frame structure: (a) Typical plan (b) Elevation (c) Base isolators (d) Storey isolators connected to core-wall

A. Core-tube Model

The fixed-base core-tube can be seen as coupled shear walls which bear both flexural deformation and shear deformation. So in this study, Timoshenko beam [15] is used to simulate the fixed-base core-tube taking first-order shear deformation effects into consideration. So Timoshenko beam elements are chosen to simulate the core-tube in this paper. As shown in Fig. 2, the core-tube is divided into a number of segments at each floor level.

These segments are connected at nodal points.

1. Timoshenko Beam Element

Suppose the Timoshenko beam element length is *l*, transverse displacement is *u* and bending rotation is *θ* at *x* place (as shown in Fig. 3 (a)), and simple linear shape functions $N_1=1-x/l$ and $N_1=x/l$ are used. Then the Timoshenko element's consistent mass matrix [15]-[17] is

$$M^e=\rho\begin{Bmatrix} lA/3 & 0 & lA/6 & 0 \\ 0 & lI/3 & 0 & lI/6 \\ lA/6 & 0 & lA/3 & 0 \\ 0 & lI/6 & 0 & lI/3 \end{Bmatrix} \qquad (1)$$

where ρ is the density of the core-tube, *A* is the section area and *I* is the moment of inertia.
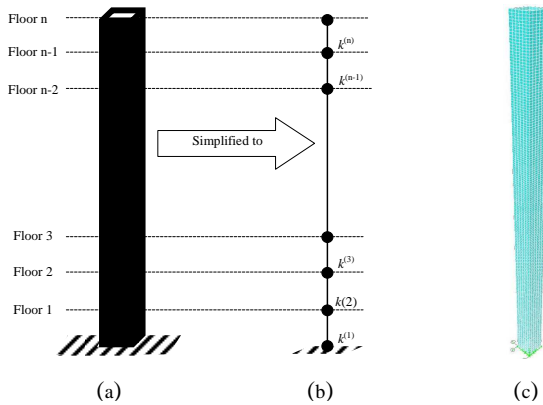
(a)　　　　　(b)　　　　　(c)

Fig. 2 Core-tube and simulation model: (a) Core-tube (b) Timoshenko beam model (c) Model in ETABS

Element stiffness matrix [15]-[17] is

$$K^e = K_b^e + K_s^e \qquad (2)$$

Where $K_b^e = EA/l \begin{Bmatrix} 0 & 0 & 0 & 0 \\ 0 & 1 & 0 & -1 \\ 0 & 0 & 0 & 0 \\ 0 & -1 & 0 & 1 \end{Bmatrix}$ is stiffness related to

bending deformation.

$$K_s^e = \mu GA \begin{Bmatrix} 1/l & 1/2 & -1/l & 1/6 \\ 1/2 & l/4 & -1/2 & l/4 \\ -1/l & -1/2 & 1/l & -1/2 \\ 1/6 & l/4 & -1/2 & l/4 \end{Bmatrix}$$ is stiffness related to

shear deformation.

where E is Young's modulus, G is shear modulus and μ is the shear coefficient of the Timoshenko beam [15]-[17]. For thin walled hollow rectangular section, the shear coefficient is

$$\mu = \frac{10(1+\nu)(1+3m)^2}{p_1 + \nu p_2 + 10mn^2(3+\nu+3m)}$$ in which ν is the Poisson

ratio [18, 19]. The two coefficients p_1 and p_2 can be calculated by the following two equations [19]:

$$p_1 = 12 + 72m + 150m^2 + 90m^3 \qquad (3)$$

$$p_2 = 11 + 66m + 135m^2 + 90m^3 \qquad (4)$$

Where coefficient m equals to $\dfrac{t_x(l_y - t_y)}{t_y(l_x + t_x)}$ and coefficient

n equals to $\dfrac{l_y - t_y}{l_x + t_x}$ in which t_x, t_y, l_x, t_x are section sizes

as shown in Fig. 3 (b). In this study, thickness of the coretube is 0.4 m.
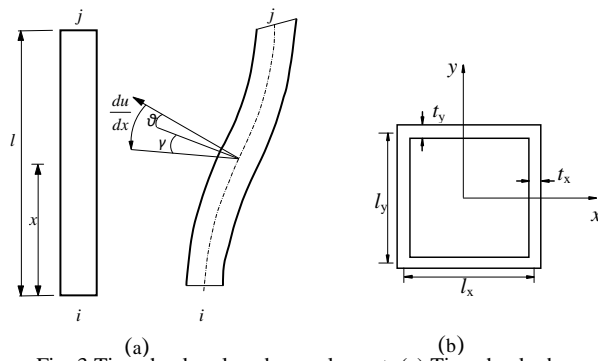

(a)　　　　　　　　　(b)

Fig. 3 Timoshenko plane beam element: (a) Timoshenko beam element (b) Timoshenko beam section

2. Equations of Motion of Core-tube

The vertical Timoshenko beam elements are assembled to yield the following equations of motion [16, 20]:

$$M_c \ddot{X}_c + C_c \dot{X}_c + K_c X_c = -M_c I_c \ddot{x}_g \qquad (5)$$

Where $\ddot{X}_c$, $\dot{X}_c$ and X_c are acceleration vector, velocity vector and displacement vector of the core-tube, respectively. Subscript c denotes core-tube.

M_c, C_c and K_c are mass matrix, damping matrix and stiffness matrix of core-tube, respectively.

$\ddot{x}_g$ is the ground acceleration.

Position vector $I_c = (1,0,1,0\cdots1,0)^T$.

Rayleigh damping is adopted with the first and second modal damping ratios ξ_c at 0.03.

Seismic response of the core-tube (e.g. acceleration, velocity, and displacement at any time t) can be obtained by solving (5) using the Newmark-β method [21]. The numerical procedure has been programmed using MATLAB software by the authors.

3. Model Validation

To verify the reliability of the Timoshenko beam model, dynamic response of a 90m high core-tube subjected to El Centro earthquake is calculated by using the above equations and compared with the results in ETABS. Shell elements are used to simulate the core-tube in ETABS as shown in Fig. 2 (c). The maximum shell element size is 0.833m×0.5m. Table 1 compares the periods and the maximum displacements computed by the two methods.

The maximum difference is less than 1%. As shown, Timoshenko beams can be used to simulate fixed-base core-tube with high accuracy.

TABLE I
PERIODS, DISPLACEMENTS COMPARISON

	Timoshenko Beam Model	ETABS	Error
Fundamental period(s)	1.9487 m	0.929	0.22%
Second period(s)	0.3230m	0.322	0.45%
Maximum top floor displacement	0.4121m	0.412	-0.08%
Minimum top floor displacement	-0.3746m	-0.375	0.00%

B. Base-isolated frame model

The base-isolated frame is modeled by a multi-degrees-of-freedom floor shear model. Masses and lateral stiffness are given in Table 2. The masses are assumed to be lumped at each floor level.

Natural rubber bearings and lead rubber bearings are used as base isolators in this paper. Lateral stiffness at base isolation layer is the sum of the lateral stiffness of total natural rubber bearings and the total initial stiffness of lead rubber bearings or the sum of the lateral stiffness of total natural rubber bearings and the total post-yield stiffness of lead rubber bearings. Fig.4 (a) shows a typical hysteresis loop of a natural rubber bearing subjected to sinusoidal force. The equivalent damping ratio for natural rubber bearings is assumed to be 3%. Lead rubber bearings are modeled by bilinear models [22, 23]. As shown in Fig. 4 (b), the properties of the lead rubber bearings are defined by 3 parameters: total lead rubber bearings yield force f_y, total initial shear stiffness k_1 and post yield shear stiffness k_2. Total initial shear stiffness of the lead rubber bearings is assumed to be 10 times the post-yield stiffness [24] which means $k_1=10k_2$ in this paper. The frame's lateral stiffness is provided by axially inextensible columns and is calculated by D-value method [25].

TABLE II
MASSES AND LATERAL STIFFNESS AT EACH FLOOR LEVEL

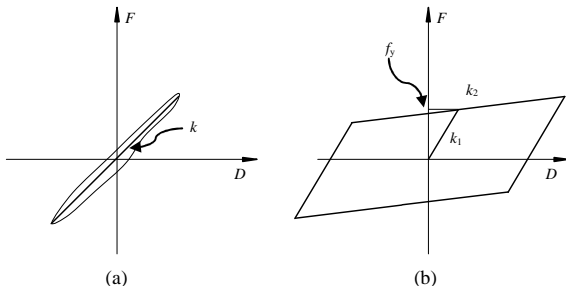|	Mass (ton)	Lateral Stiffness (MN/m)
Ground floor	1.04976×10^3	Total base isolator stiffness
Other floors	1.17936×10^3	2.211×10^3
Top floor	1.04976×10^3	2.211×10^3

Fig. 4 Models of natural rubber bearings and lead rubber bearings:
(a) Hysteretic shape of natural rubber bearings (b) Bilinear model of lead rubber bearings

Equations of motion [20] of the base-isolated frame can be written in the following form:

$$M_f \ddot{X}_f + C_f \dot{X}_f + K_f X_f + R_L = -M_f I_f \ddot{x}_g \quad (6)$$

Where $\ddot{X}_f$, $\dot{X}_f$ and X_f are acceleration vector, velocity vector and displacement vector of the base-isolated frame, respectively.

Subscript f denotes the frame.

R_L is a vector representing the nonlinear restoring force of the lead rubber bearings at base isolation level.

I_f is a unit vector.

M_f, C_f and K_f are mass matrix, damping matrix and stiffness matrix of the base-isolated frame, respectively.

$$M_f = \begin{Bmatrix} m_1 & 0 & \cdots & 0 \\ 0 & m_2 & \cdots & 0 \\ \vdots & \vdots & \ddots & 0 \\ 0 & 0 & 0 & m_{30} \end{Bmatrix} \quad (7)$$

Where $m_1, m_2 \ldots, m_{30}$ are masses at each floor level.

$$\{K\}_f = \begin{Bmatrix} k_2+k_{NRB} & -k_2 & 0 & \cdots & 0 \\ k_2 & k_2+k_3 & -k_3 & \cdots & 0 \\ 0 & -k_3 & k_3+k_4 & \cdots & 0 \\ \vdots & \vdots & \vdots & \ddots & 0 \\ 0 & 0 & 0 & 0 & k_{30} \end{Bmatrix} \quad (8)$$

Where k_{NRB} is the total natural rubber bearing stiffness at isolation layer and $k_2, k_3 \ldots, k_{30}$ are lateral stiffness at each floor level.

Rayleigh damping is adopted for the frame above isolation layer with the first and second modal damping ratios ξ_{NRB} at 0.03. Stiffness proportional damping is adopted at isolation layer (i.e. $\dfrac{2\xi_{NRB}}{\omega_{isolation}}k_{NRB}$). Total base isolator stiffness is used to calculate the first circular frequency of the base-isolated frame $\omega_{isolation}$.

C. Model of the proposed structural system and equations of motion

Fig. 5 shows the simplified analytical model of the proposed structural system. The core-tube is modeled by a vertical cantilevered beam and the base-isolated frame is modeled by floor shear model. Lead rubber bearings are designed as storey isolators to connect the frame and core-tube as well as to absorb energies. These storey isolators are simulated by bilinear model.

Equations of motion [20] of the proposed structural system as shown in Fig. 5 are in the form of:

$$M\ddot{X} + C\dot{X} + KX + R_{LRB} = -MI\ddot{x}_g \quad (9)$$

Where mass matrix $M = \begin{Bmatrix} M_c & 0 \\ 0 & M_f \end{Bmatrix}$ and damping matrix $C = \begin{Bmatrix} C_c & 0 \\ 0 & C_f \end{Bmatrix}$.

R_{LRB} is a vector representing the nonlinear restoring force of the lead rubber bearings at base isolation layer.

Position vector $I = \begin{Bmatrix} I_c \\ I_f \end{Bmatrix}$.

Stiffness matrix $K = \begin{Bmatrix} K_c + K_c^{si} & K^{si} \\ K^{si} & K_f + K_f^{si} \end{Bmatrix}$ in which K_c^{si},

K^{si} and $K_{\mathrm{f}}^{\mathrm{si}}$ are three components and superscript si denotes storey isolators.

These three storey stiffness matrix can be calculated by the following three equations:

$$\{K\}_{\mathrm{c}}^{\mathrm{si}} = \begin{Bmatrix} k_{\mathrm{si}} & 0 & 0 & 0 & \cdots & 0 & 0 \\ 0 & 0 & 0 & 0 & \cdots & 0 & 0 \\ 0 & 0 & k_{\mathrm{si}} & 0 & \cdots & 0 & 0 \\ 0 & 0 & 0 & 0 & \cdots & 0 & 0 \\ \vdots & \vdots & \vdots & \vdots & \ddots & 0 & 0 \\ 0 & 0 & 0 & 0 & 0 & k_{\mathrm{si}} & 0 \\ 0 & 0 & 0 & 0 & 0 & 0 & 0 \end{Bmatrix}_{60\times60} \qquad (10)$$

Where k_{si} is the total storey isolator stiffness at each floor level. It should be noted that k_{si} equals to the initial stiffness of the total storey isolators when in elastic region and equals to the post-elastic stiffness of the total storey isolators when in post-elastic region.

$$\{K\}^{\mathrm{si}} = \begin{Bmatrix} k_{\mathrm{si}} & 0 & \cdots & 0 & 0 \\ 0 & 0 & \cdots & 0 & 0 \\ 0 & k_{\mathrm{si}} & \cdots & 0 & 0 \\ 0 & 0 & \cdots & 0 & 0 \\ \vdots & \vdots & \ddots & \vdots & \vdots \\ 0 & 0 & \cdots & k_{\mathrm{si}} & 0 \\ 0 & 0 & \cdots & 0 & 0 \end{Bmatrix}_{60\times30} \qquad (11)$$

$$\{K\}_{\mathrm{f}}^{\mathrm{si}} = \begin{Bmatrix} k_{\mathrm{si}} & 0 & \cdots & 0 \\ 0 & k_{\mathrm{si}} & \cdots & 0 \\ \vdots & \vdots & \ddots & \vdots \\ 0 & 0 & \cdots & k_{\mathrm{si}} \end{Bmatrix}_{30\times30} \qquad (12)$$
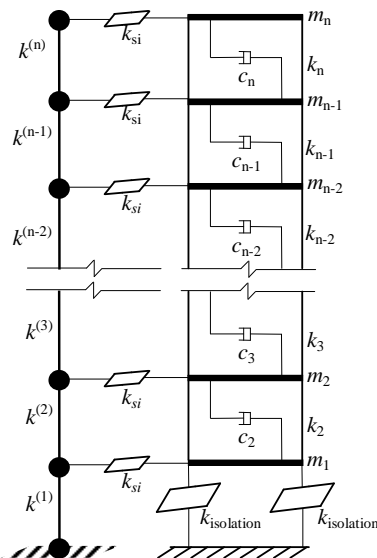

Fig. 5 Analytical model

Since bilinear model is used to simulate lead rubber bearings, it is more convenient to rewrite (9) in incremental form:

$$M\Delta\ddot{X} + C\Delta\dot{X} + K\Delta X + \Delta R = -MI\Delta\ddot{x}_g \qquad (13)$$

Where $\Delta\ddot{X}$, $\Delta\dot{X}$, ΔX and $\Delta\ddot{x}_g$ are respective system's acceleration increment vector, velocity increment vector, displacement increment vector, and ground acceleration increment. All elements of ΔR equal to zero except the 61th one Δr which represents restoring force increment. The restoring force Δr equals to $k_{\mathrm{LRB}}\Delta x_{\mathrm{isolation}}$ and k_{LRB} equals to initial stiffness when the lead rubber bearings at isolation layer are elastic and post-yield stiffness when the lead rubber bearings at isolation layer are in the post-elastic region. $\Delta x_{\mathrm{isolation}}$ is displacement increment of the isolated frame at base isolation layer.

Equation (13) is solved using the Newmark-β method [21], and responses (e.g. acceleration, velocity and displacement) at any time t can be obtained numerically. In the analysis, center core and frames are assumed to behave linearly elastic throughout the loading history and lead rubber bearings behave nonlinearly by bilinear model.

IV. EARTHQUAKES INPUT AND ISOLATOR PARAMETERS

A. Earthquakes input

The building group is assumed to be located in a medium soft area with seismic intensity at the VIII degree in accordance with the Chinese code [26]. Three earthquakes used in this paper are the I-ELC180 component of Imperial Valley 1940 earthquake recorded at El Centro, TAF111 component of Kern County 1952 earthquake recorded at Taft Lincoln School, TAZ090 component of Kobe 1995 earthquake recorded at Takarazuka station, respectively. Peak ground accelerations of the earthquake records are scaled to 4m/s2 representing rarely occurred earthquakes.

B. Base isolators and story isolators

Fig. 6 shows the displacement response spectra at 5% damping ratio. It's observed that for Kobe earthquake the suitable period is larger than 4 seconds, for El Centro earthquake the suitable period is around 4.8 seconds, and for Taft earthquake the displacement response remains stable when period varies from 2 seconds to 4.2 seconds. From the above observation, it is concluded that the suitable period is around 4 seconds.

In order to set the fundamental period of the system around suitable period 4 seconds, 28 LNR-D1200 isolators and 4 LRB-D1200 isolators are designed to act as base isolators and 124 LRB300-60 isolators are used as story isolators as shown in Table 3 and Fig. 1 (c). When the initial stiffness of all lead rubber bearings is used the fundamental period of the system is 3.22 seconds, and when the yielded stiffness of all lead rubber bearings is used the fundamental period of the system is 4.77 seconds. For equivalent stiffness of the lead rubber bearings, the system's fundamental period is around 4.23 seconds.
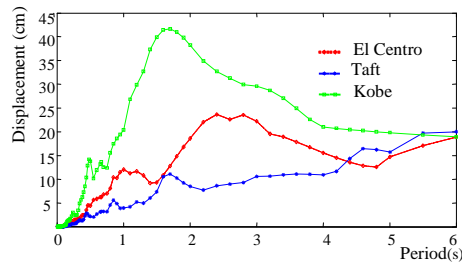
Fig. 6 Displacement response spectra for the three design earthquakes at 5% damping ratio

TABLE III
MECHANICAL PROPERTIES OF ISOLATORS

	k_1 (MN/m)	k_2 (MN/m)	f_y (kN)	Capacity (MN)	Total Amount
LNR-D1200	1.838	-	-	16.965	28
LRB-D1200	18.78	1.878	360.8	16.965	4
LRB300-60	4.35	0.435	25.48	0.707	124

V. RESULTS AND COMPARISON

Equation (16) is solved by Newmark-β method in MATLAB. In consideration of the nonlinear properties of the base isolators, small time interval $\Delta t = 0.01/100 = 1 \times 10^{-4}$ s is used.

A. Results of analysis

Fig. 7 shows the maximum drift of the core-tube and the frame at each floor level. Maximum drifts of the core-tube occur at the top floor level. The maximum drifts of the core-tube under the three earthquakes are 11.58mm, 12.02mm and 8.54mm. The corresponding storey drift angles are 1/259, 1/250 and 1/351, respectively.

The maximum drifts of the frame occur around the middle of the frame and the values are 5.05mm, 6.16mm and 6.53mm. Corresponding storey drift angles are 1/594, 1/487 and 1/459, respectively.

Fig. 8 shows the maximum relative displacement between the core-tube and the frame at each floor level. The maximum relative displacement between the core-tube and the frame occur around the fourth floor level. The maximum values are 129.16mm, 140.92 mm and 90.50 mm under the three earthquakes, respectively. These values are less than the design seismic joint width at 311.5 mm according to Chinese Code for Seismic Design of Buildings [26].
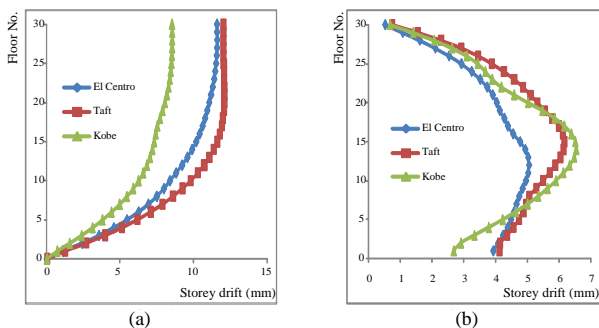

Fig. 7 Maximum story drifts: (a) Core-tube (b) Frame

Fig. 9 shows the maximum relative displacement of the frame with respect to ground. It is observed that the maximum displacement occurs at the top floor level and more than 50% of the largest displacement occurs at base level. The maximum displacements at the base are 122.68 mm, 134.89 mm and 87.29 mm, respectively. These values are far less than the displacement limit of the base isolators which is 660 mm.
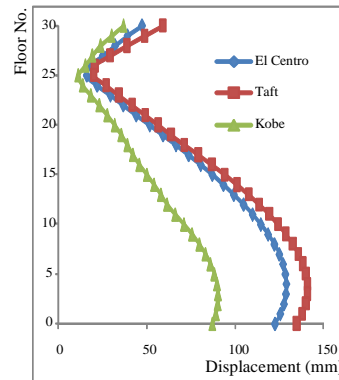

Fig. 8 Maximum relative displacement between the core-tube and the frame against floor level
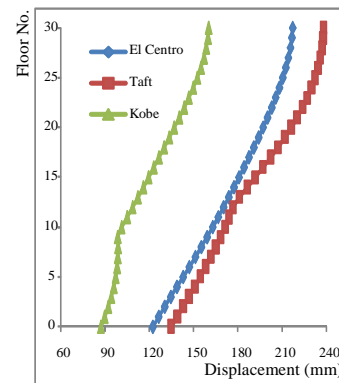

Fig. 9 Maximum displacement against floor level

B. Comparisons

Fig. 10 shows the ETABS model of the fixed-base tube-frame structure corresponding to the structural system studied in this paper. This system is similar to the above mentioned new tube-frame system but without any base isolators and any story isolators. The fundamental period of this building is 2.237s. It should be noted that in the ETABS model, the damping ratio for the ith mode is defined as $\xi_i = \alpha/(2\omega_i) + \beta\omega_i/2$ in which ω_i is the circular frequency of the ith mode and α and β are two coefficients for Rayleigh damping [20].

Table 4 compares the maximum base shear, maximum drift and maximum acceleration of the new system with those obtained from corresponding fixed-base earthquake resistant system by ETABS. The following can be observed: the maximum base shear is reduced by more than 65%, the maximum drift is reduced by more than 55%, and the maximum acceleration is reduced by more than 80%. As

compared with the fixed-base building, the new structural system shows substantial reduction on structural response to earthquake motion.

TABLE IV
RESPONSE COMPARISON

		Fixed Tube-frame	Proposed System	Percentage Reduction
Maximum base shear	El Centro	72.01 MN	20.70 MN	71.25%
	Taft	62.92 MN	20.99 MN	66.64%
	Kobe	59.90 MN	15.68 MN	73.82%
Maximum drift	El Centro	22.06 mm	5.05 mm	77.11%
	Taft	15.63 mm	6.16 mm	60.58%
	Kobe	15.00 mm	6.53 mm	56.47%
Maximum acceleration	El Centro	7.67 m/s^2	1.156 m/s^2	84.93%
	Taft	8.43 m/s^2	1.552 m/s^2	81.60%
	Kobe	7.56 m/s^2	1.372 m/s^2	81.84%

VI. CONCLUSIONS

Energy dissipation systems, seismic isolation system and suspension systems have their individual unique features. These three systems have been studies by tremendous researchers and there are many successful applications in the past decades. Incorporating the merits of these three systems, a new earthquake resistant system namely composite fixed-base core-tube and base-isolated frame structural system is proposed in this paper. Base isolators are selected according to the displacement response spectra for three design earthquake waves and are designed to protect the frame from strong earthquakes. Story isolators are designed to provide lateral resistance and dissipate energy from serious earthquakes or winds. Equations of motion are formulated to study the response of the new system to strong earthquake motions. As compared with the corresponding fixed-base building, the new earthquake resistant system shows substantial reduction on structural response to earthquake motions.

REFERENCES

[1] M. D. Symans, F. A. Charney, A. S. Whittaker, M. C. Constantinou, C. A. Kircher, M. W. Johnson and R. J. McNamara, Energy Dissipation Systems for Seismic Applications: Current Practice and Recent Developments, J. Struct. Eng. 2008; 134(1) 3-21.

[2] M.C. Constantinou, P.Tsopelas, W. Hammel and A.N. Sigaher, Toggle-brace-damper seismic energy dissipation system, J. Struct. Eng. 2001; 127(2) 105–112.

[3] T.S.K. Chung, E.S.S. Lam, B.Wu and Y.L. Xu, Retrofitting Reinforced Concrete Beam-column Joints by Hydraulic Displacement Amplification Damping System. Proceedings of 2007 ASCE Structures Congress. Long Beach, California; 2007.

[4] A. Whittaker and M. Constantinou, Seismic Energy Dissipation Systems for Buildings, in: Y. Bozorgnia, V.V. Bertero (Eds.), Earthquake Engineering From Engineering Seismology to Performance-Based Engineering, Taylor & Francis, London, 2006, pp. 716-744.

[5] J.M. Kelly, Aseismic base isolation: review and bibliography, Soil Dyn. Earthq. Eng.1986; 5(4) 202-216.

[6] R.L. Mayes and F. Naeim, Design of Structures with Seismic Isolation, in: F. Naeim (Eds.), The Seismic Design Handbook, second ed., Kluwer academic publishers, Boston, Dordrecht, London, 2001, pp.723-756.

[7] H.N. Li and X.X. Wu, limitations of height to width ratio for base-isolated buildings under earthquake, Struct. Design Tall Spec. Build. 2006; 15 277–287.

[8] T. Komuro, Y. Nishikawa, Y. Kimura and Y. Isshiki, Development and realization of base isolation system for high-rise buildings, J. Adv. Concr. Technol. 2005; 3(2) 233-239.

[9] L. Bo, S.S. Xiong and J.X. Tang, Wind effects on habitability of base-isolated buildings, J. Wind Eng. Ind. Aerodyn.2002; 90 1951–1958.

[10] M. Mezzi and A. Parducci, Conceptual seismic design and state-of-the art protection systems. 8th U.S. National Conference on Earthquake Engineering. San Francisco, California, USA; April 2006.

[11] Y. Nakamura, M. Saruta, A. Wada, T. Takeuchi, S. Hikone and T. Takahashi, Development of the core-suspended isolation system, Earthq. Eng. Struct. D. 2011; 40:429–447.

[12] D. Mar, L. Panian, R.A. Dameron, B.E. Hansen, S. Vahdani, D, Mitchell and J. Paterson, Performance-based seismic upgrade of a 14-story suspended slab building using state-of-the-art analysis and construction techniques, Proceedings of SEAOC 69th Annual Convention, Sacramento, California; 2000, pp.127–142.

[13] D. Mar, and S. Tipping, Smart frame story isolation: a new high-performance seismic technology, 9th U.S.-Japan Workshop on the Improvement of Structural Design and Construction Practices, Victoria, British Columbia, Canada, 2000.

[14] J.E. LUCO AND F.C.P. DE Barros, Control of the seismic response of a composite tall building modelled by two interconnected shear beams, Earthq. Eng. Struct. 27(1998) 205-223.

[15] P. S. Timoshenko and M.J. Gere, Theory of Elastic Stability, McGraw-Hill, New York, 1961.

[16] K.K. Kapur, Vibrations of a Timoshenko Beam, Using Finite-Element Approach, J. Acoust. Soc. Am. 40 (1966) 1058–1063.

[17] K.J. Bathe, Finite Element Procedure, Prentice-hall, Upper Saddle River, New Jersey, 1996.

[18] I. A. Karnovsky and O. I. Lebed, non-classical vibration of arches and beams: Eigenaluves and Egenfunctions, McGraw-hill, New York, 2004.

[19] Hutchinson, J.R. (2001), Shear Coefficients for Timoshenko Beam Theory, J. Appl. Mech., 68(1), 87-92.

[20] A.K. Chopra, Dynamics of structures: theory and applications to earthquake engineering, Upper Saddle River, New Jersey, 1995.

[21] T.K. Datta, Seismic analysis of structures,John Wiley & Sons (Asia) Pte Ltd., Singaore, 2010.

[22] H. Fujitani and T. Saito, Devices for aeismic isolation and response control, in: M. Higashino, and S. Okamoto (Eds.), Response Control and Seismic Isolation of Buildings, Taylor & Francis, London and New York, 2006, pp.3-37.

[23] C.P. Providakis, Effect of LRB isolators and supplemental viscous dampers on seismic isolated buildings under near-fault excitations, Eng. Struct. 30(2008) 1187–1198.

[24] P. Komodromos, Seismic isolation for earthquake-resistant structures, WIT press, Ashurst Lodge, Ashurst, Southampton, SO40 7AA, UK, 2000.

[25] W.X Cheng, D.H. Yan, G.Y. Kang and J.J. Jiang, Concrete structure Part II: concrete structure design, China architecture & building press, Beijing, 2003.

[26] GB50011–2010, Code for seismic design of buildings, Chinese Architecture & Building Press, Beijing, 2010.